PAPER • **OPEN ACCESS**

Monitoring The Sea Surface Temperature and Total Suspended Matter Based on Cloud-Computing Platform of Google Earth Engine and Open-Source Software

To cite this article: F Ramdani *et al* 2021 *IOP Conf. Ser.: Earth Environ. Sci.* **750** 012041

Monitoring The Sea Surface Temperature and Total Suspended Matter Based on Cloud-Computing Platform of Google Earth Engine and Open-Source Software

F Ramdani[1,*], A Wirasatriya[2], A R Jalil [3]
[1] Geoinformatics Research Group, Faculty of Computer Science, Brawijaya University, Malang, Indonesia.
[2] Department of Oceanography, Faculty of Fisheries and Marine Science, Universitas Diponegoro, Tembalang Campus, St. Prof. Soedarto S.H., Semarang, Central Java Indonesia.
[3] Faculty of Marine Science and Fisheries, Department of Marine Science, Hasanuddin University, Makassar, South Sulawesi, Indonesia

Email: fatwaramdani@ub.ac.id

Abstract. The sea surface temperature and total suspended matter is important for fisheries industry to increase the opportunity to catch the fish. Traditional methods to monitor this phenomenon is by using the remote sensing techniques. However, conventional remote sensing methods is need higher computer specifications as well as larger space of hard disk drive and commercial software to process the datasets. The availability of cloud-computing platform such as Google Earth Engine that available free for public will provide benefit for researcher to increase the efficiency and effectivity of large-scale imageries processing. This study proposed the sate-of-the-art cloud-computing platform of GEE to monitor and map the sea surface temperature and total suspended matter for long periods of analysis of Timor Sea, Van Diemen Gulf, and Beagle Gulf, Australia. In total there more than 600 images of Landsat 8 Collection 1 Tier 1 calibrated top-of-atmosphere (TOA) reflectance is used and obtained within the GEE platform. The Radiative transfer equation (RTE) method is used to extract the surface temperature. To extract the total suspended matter, the Sentinel-3 Ocean and Land Color Instrument Earth Observation Full Resolution (OLCI EFR) is used. The Case-2 Regional CoastColour (C2RCC) processor within the SentiNel Application Platform (SNAP) software is used. The result show that the GEE platform is successfully captured the dynamic sea surface temperature as well as the total suspended matter with high efficiency in term of time and hard disk drive consumption.

1. Introduction

According to the FAO report [1], the sea surface temperature of global open ocean has been increased around 0.11°C per decade on average, while the coastal areas have been increased around 0.18±0.16°C per decade on average. This situation is likely to cause the fluctuations of the fisheries production. The tropical regions will face decrease up to 40%, while the high latitude regions could increase the marine capture fisheries around 30% to 70% [1]

One of many variables that influence the fisheries productions is sea surface temperatures. Some researchers have been tried to utilized the medium and higher spatial resolution to produce sea surface temperature such as MERIS and Landsat images. For instance, research by Uiboupin et al [2] monitor the upwelling events in the Gulf of Finland using MERIS images. They compared the surface temperature with the chlorophyll *a* (Chl *a*) distribution and found the consistent relation between those parameters. Meanwhile, Aleskerova et al [3] retrieved sea surface

temperature of Black Sea using Landsat-8 and two-channel method. They found that the result of Landsat-8 and MODIS images only have small differences in surface temperature mapping, it is around 0.58°C.
However, the previous studies have also shown that the procedure to retrieved sea surface temperature is need large size of satellite image, high computer specification, and utilization of commercial software. This traditional method is considered as time-consuming and costly method. The objective of this study is to propose new method based-on cloud-computing geocomputation platform of Google Earth Engine (GEE) to retrieve sea surface temperature information from thermal channel of Landsat-8.
GEE is cloud-computing platform to process large scale satellite images that available free for public [4]. Over twenty petabyte of satellite imagery and geospatial datasets is available for everyone to analyses and monitor the earth's surface. To operate the GEE platform, we need to work based on code editor using JavaScript. The GEE platform could be accessed through http://code.earthengine.google.com/
Some researchers have been used the GEE platform to analyses the land cover mapping [5], annual irrigation [6], wetland inventory [7], mapping particulate matter [8], mapping shorelines [9], and mapping wetland [10]. However, based on our current knowledge, there is very limited research using GEE to monitor the sea surface temperature and total suspended matter.
Therefore, this study will provide the first detailed record of total suspended matter and the sea surface temperature information around Timor Sea, Van Diemen Gulf, and Beagle Gulf. Seven years of Landsat-8 observation, from 2013-2020 is used with special focus in the August 2016. In Section II the materials and methods are explained, the main result and analysis follow in Section III. Finally, Section IV consists of summary of the study and conclusions.

2. Material and Methods

2.1 Study area

The study area is northern part Australia. There are three main locations selected to retrieve the sea surface temperature and total suspended matter as shown in Figure. 1. The first location is Van Diemen Gulf (red colour), the second location is Beagle Gulf (yellow colour), and the last location is Timor Sea (blue colour)
These locations is selected due to high amount of total suspended matter reported by some scientific resources on different periods of analysis [11]–[14].

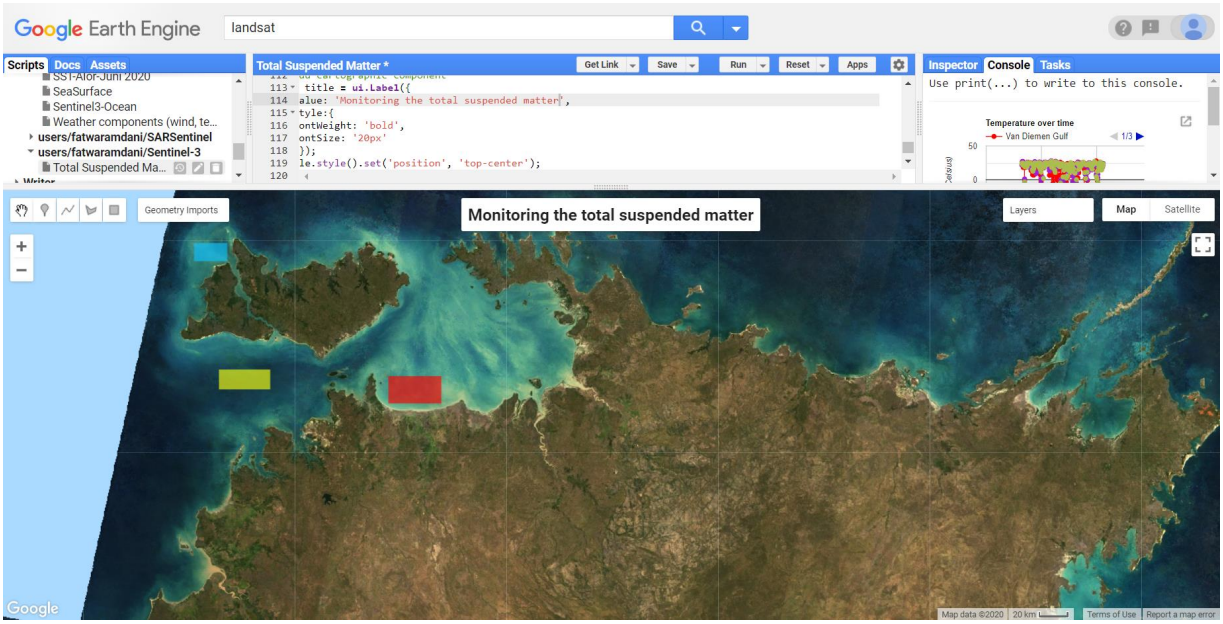

Figure 1. Study area as shown within the GEE paltform

2.2 Imagery datasets

The Landsat 8 Collection 1 Tier 1 calibrated top-of-atmosphere (TOA) reflectance is used and obtained within the GEE platform. This dataset is corrected version (Level 1T – Terrain corrected). Landsat 8 has two channels of Thermal Infrared Sensor (TIRS), that is Band 10 (B10) and Band 11 (B11) with wavelength 10.9 (10.6-11.2) and 12.0 (11.5-12.5) μm, respectively. The original resolution of TIRS bands is 100 m and have been resampled to 30 m spatial resolution [15]. In total more than 600 images were processed for an approximately 350 by 260 km subset covering the study area in the periods from early May 2013 to end of July 2020 from the two WRS-2 path/row (105/68 and 106/68) tile set covering the study area.

2.3 Sea surface temperature extraction

Radiative transfer equation (RTE) method is chooses based on the research by reference [16]. They research found that when using Landsat 8 Thermal Infrared Sensor (TIRS) data, RTE method produced the best results compared to Mono Window Algorithm (MWA) and Single-Channel Algorithm (SCA).

RTE method is a straightforward technique to produce surface temperature from a single TIR band. In this study we used band 10 of Landsat 8 to retrieve sea surface temperature. Since based on the research by Vanhellemont [17] band 10 has lower Root Mean Squared Difference (RMSD) of 0.7 Kelvin, compared to band 11 with 1 Kelvin RMSD.

To produce the sea surface temperature from band 10 we need to convert the digital number(s) into radiance and then convert the radiance into top of atmosphere brightness temperature. The equation to convert digital number(s) into radiance is as shown in equation (1)[18]

$$L_\lambda = M_L * Q_{cal} + A_L L_\lambda = M_L * Q_{cal} + A_L \qquad (1)$$

Where:

$L_\lambda L_\lambda$ = Spectral radiance (W/(m2*srad*μm)

$M_L M_L$ = Radiance multiplicative scaling factor for the band (RADIANCE_MULT_BAND_10 from the metadata)

$A_L A_L$ = Radiance additive scaling factor for the band (RADIANCE_ADD_BAND_10 from the metadata)

$Q_{cal} Q_{cal}$ = Level-1 pixel value in digital number (DN)

To convert the spectral radiance into top of atmosphere brightness temperature, the equation formula is shown in equation (2)[19]

$$T = \frac{K_2}{ln\left(\frac{K_1}{L_\lambda}+1\right)} T = \frac{K_2}{ln\left(\frac{K_1}{L_\lambda}+1\right)} \qquad (2)$$

Where:

TT = Top of atmosphere brightness temperature (Kelvin)

$L_\lambda L_\lambda$ = Spectral radiance (W/(m2*srad*μm)

$K_1 K_1$ = Band 10 of L8 constants (774.89)

$K_2 K_2$ = Band 10 of L8 constants (1321.08)

Finally, to convert the top of atmosphere brightness temperature into degree Celsius, the equation (3) formula is used

$$Celsius = K - Celsius = K - 273 \qquad (3)$$

Where:

K = Temperature in Kelvin

$L_\lambda Celsius$ = Temperature in Celsius

2.4 Validation

The Sentinel-3 Ocean and Land Color Instrument Earth Observation Full Resolution (OLCI EFR) is used to validate the total suspended matter of the study area. The Sentinel-3 OLCI EFR is designed to retrieve the spectral distribution of upwelling radiance just above the sea surface [20].

There are 21 spectral bands of Sentinel-3 OLCI EFR with 300m spatial resolution and repeated cycle time every 2 days. The wavelength is ranging between 0.4µm and 1.02µm [21]. To visualize the natural colour, we could use RGB combination of Oa08_radiance, Oa06_radiance, and Oa04_radiance, respectively.

The Sentinel-3 OLCI EFR is also available within the GEE platform. The availability is since August, 2016 to present day.

The Sentinel-3 OLCI is also available to download from the URL https://scihub.copernicus.eu/dhus/#/home. We then processed the Level-1 OLCI EFR datasets using Case-2 Regional CoastColour (C2RCC) Processor within the SNAP software to retrieved the total suspended matters. This processor performs atmospheric correction and inherent optical properties (IOP) retrieval on Sentinel-3 OLCI Level-1 data. The result then converted into GeoTIFF to process within the QGIS software. We used band subset to choose only *conc_tsm* data that need to be exported into GeoTIFF.

3. Results and Discussion

The sea surface temperature of the study area during the periods of analysis is shown in Figure. 2. We exclude the temperature below 10°C since we assumed it was cloud cover. In total there are more than 125 of 650 images were excluded from the analysis due to very low surface temperature.

The trend of sea surface temperature during period of analysis is very dynamic. We found the low sea surface temperature is occurred every March to August each year. While the higher sea surface temperature is occurred every September to November, and it became low again during December to February, however it is still higher than periods of March to August.

Our study also found that the year 2015 and 2019 are the hottest year compared to other period of analysis. From January to December of 2015 and 2019, the average sea surface temperature of the study areas is higher than other periods of analysis, in average 22.7°C and 22.4°C respectively. Year 2016 is selected since it shows the lowest average sea surface temperature, 20°C. While August 2016 is selected due to that month show clear cloud coverage and has the lowest average temperature of 18.3°C.

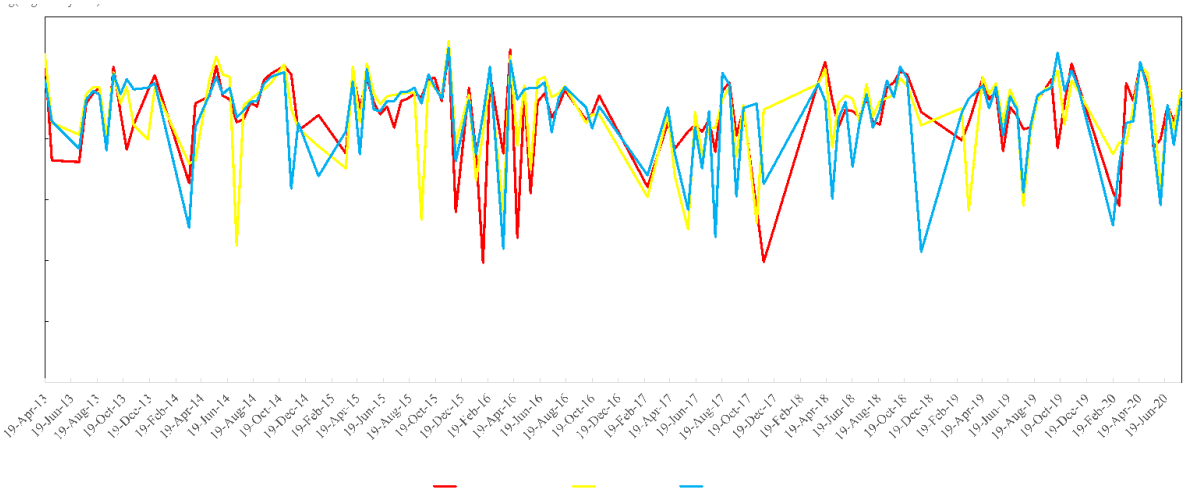

Figure 2. The surface temperature (SST) of three study areas from 2013 to 2020

After we validated the low sea surface temperature of August 2016 with the Sentinel-3 OLCI EFR datasets we found positive result. The result of Sentinel-3 OLCI EFR found high concentration of total suspended matter (Figure 3) during the low sea surface temperature event. Therefore, we could conclude that even in low sea surface temperature the suspended matter is still can be found.

The result of this study is consistent with the research by Blondeau-Patissier [14] and Schroeder et al [12] who used different satellite sensor and remote sensing technique of the same study area. The total suspended matter is relatively high in dry season due to tidal-driven resuspension amplified by wind and low in wet season due to river run-off into the Van Diemen Gulf is filtered by the wetland of Kakadu National Park.
Our study found that the maximum total suspended matter in August 2016 was ranging between 200-300 g m-3, while the minimum average values ranging between 50-100 g m-3. The code is available here https://code.earthengine.google.com/?scriptPath=users%2Ffatwaramdani%2FSentinel-3%3ATotal%20Suspended%20Matter while the final result is also published in the form of web apps (WebGIS) and can be accessed through the url https://fatwaramdani.users.earthengine.app/view/total-suspended-matter

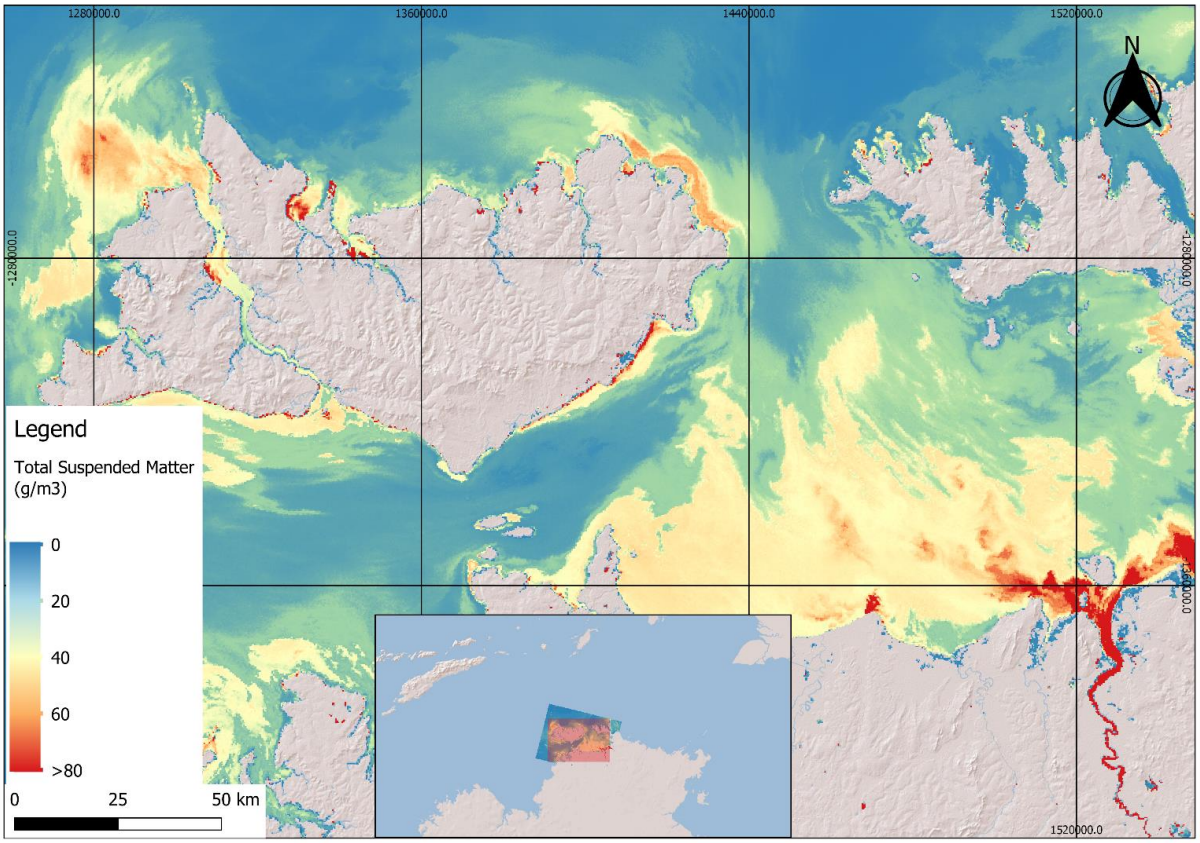

Figure 3. The map of total suspended matter (TSM) of the study areas.

4. Conclusion

This study evaluated the extraction of sea surface temperature and total suspended matter using TIR band of Landsat-8 and Sentinel-3 around Van Diemen Gulf, Beagle Gulf, and Timor Sea. Cloud-computing platform of GEE was used for seven years periods of analysis. More than 600 images of TIR band of Landsat-8 were acquired. Due to cloud cover, more than 125 images were excluded from the analysis. The excluded images shown very low sea surface temperature, in average below 10°C.
The obtained result showed that the sea surface temperature around the study area is dynamic along the periods of analysis. The image is clear from cloud coverage and show average sea surface temperature of ~20°C. The periods of low sea surface temperature are found from March to August each year, while the high sea surface temperature is found from September to November each year.
The result indicated that the suspended matter is always transported to the study area in every season along the years. The method used in this study shows very promising since it is very efficient and effective in term of time-consuming as well as the hard disk drive space to save hundreds of files of satellite imageries.

Acknowledgments
The author(s) thanks to *Program Penelitian Kolaborasi Indonesia* (PPKI) fiscal year 2020 to support this research. The first, second and third author thank to the Program of Indonesia Collaborative Research held by Universitas Brawijaya Diponegoro University, and Hasanuddin University with the contract no. 455.1/UN10.C10/PN/2020; no. 193.07/UN7.6.1/PP/2020; no. 1269/UN4.22/PT.01.03/2020.

References
[1] S. Anika and Y. Cassandra De, *Climate Change Implications for Fisheries and Aquaculture. Summary of the findings of the IPCC Fifth Assessment Report*, vol. **FIAP/C1122**. 2016.
[2] R. Uiboupin, J. Laanemets, L. Sipelgas, L. Raag, I. Lips, and N. Buhhalko, "Monitoring the effect of upwelling on the chlorophyll a distribution in the gulf of Finland (Baltic Sea) using remote sensing and in situ data," *Oceanologia*, vol. **54**, no. **3**, pp. 395–419, 2012, doi: 10.5697/oc.54-3.395.
[3] A. A. Aleskerova, A. A. Kubryakov, and S. V. Stanichny, "A two-channel method for retrieval of the Black Sea surface temperature from Landsat-8 measurements," *Izv. - Atmos. Ocean Phys.*, vol. **52**, no. **9**, pp. 1155–1161, 2016, doi: 10.1134/S0001433816090048.
[4] N. Gorelick, M. Hancher, M. Dixon, S. Ilyushchenko, D. Thau, and R. Moore, "Google Earth Engine: Planetary-scale geospatial analysis for everyone," *Remote Sens. Environ.*, vol. **202**, pp. 18–27, 2017, doi: 10.1016/j.rse.2017.06.031.
[5] M. Mardani, H. Mardani, L. De Simone, S. Varas, N. Kita, and T. Saito, "Integration of machine learning and open access geospatial data for land cover mapping," *Remote Sens.*, vol. **11**, no. **16**, pp. 1–17, 2019, doi: 10.3390/rs11161907.
[6] J. M. Deines, A. D. Kendall, M. A. Crowley, J. Rapp, J. A. Cardille, and D. W. Hyndman, "Mapping three decades of annual irrigation across the US High Plains Aquifer using Landsat and Google Earth Engine," *Remote Sens. Environ.*, vol. **233**, no. October, p. 111400, 2019, doi: 10.1016/j.rse.2019.111400.
[7] M. Amani *et al.*, "A generalized supervised classification scheme to produce provincial wetland inventory maps: an application of Google Earth Engine for big geo data processing," *Big Earth Data*, vol. **00**, no. 00, pp. 1–17, 2019, doi: 10.1080/20964471.2019.1690404.
[8] M. Fuentes, K. Millard, and E. Laurin, "Big geospatial data analysis for Canada's Air Pollutant Emissions Inventory (APEI): using google earth engine to estimate particulate matter from exposed mine disturbance areas," *GIScience Remote Sens.*, vol. **00**, no. 00, pp. 1–13, 2019, doi: 10.1080/15481603.2019.1695407.
[9] K. Vos, K. D. Splinter, M. D. Harley, J. A. Simmons, and I. L. Turner, "CoastSat: A Google Earth Engine-enabled Python toolkit to extract shorelines from publicly available satellite imagery," *Environ. Model. Softw.*, vol. **122**, p. 104528, 2019, doi: 10.1016/j.envsoft.2019.104528.
[10] J. N. Hird, E. R. DeLancey, G. J. McDermid, and J. Kariyeva, "Google earth engine, open-access satellite data, and machine learning in support of large-area probabilisticwetland mapping," *Remote Sens.*, vol. **9**, no. **12**, 2017, doi: 10.3390/rs9121315.
[11] Y. Sheng, D. Tang, and G. Pan, "Phytoplankton bloom over the Northwest Shelf of Australia after the Montara oil spill in 2009," *Geomatics, Nat. Hazards Risk*, vol. **2**, no. **4**, pp. 329–347, 2011, doi: 10.1080/19475705.2011.564213.
[12] T. Schroeder *et al.*, "Remote sensing methods to map and monitor the condition of coastal habitats and other surrogates for biodiversity," *CSIRO Ocean. Atmos. Flagsh.*, vol. Part B: Wa, no. March, p. 34, 2015.
[13] D. Blondeau-Patissier *et al.*, "Bio-optical properties of two neigboring coastal regions of tropical Northern Australia: The Van Diemen Gulf and Darwin Harbour," *Front. Mar. Sci.*, vol. **4**, no. MAY, pp. 1–27, 2017, doi: 10.3389/fmars.2017.00114.
[14] D. Blondeau-Patissier, T. Schroeder, V. E. Brando, S. W. Maier, A. G. Dekker, and S. Phinn, "ESA-MERIS 10-year mission reveals contrasting phytoplankton bloom dynamics in two tropical regions of Northern Australia," *Remote Sens.*, vol. **6**, no. 4, pp. 2963–2988, 2014, doi: 10.3390/rs6042963.
[15] G. Developer, "USGS Landsat 8 Collection 1 Tier 1 TOA Reflectance," *Earth Engine Data Catalog*, 2020. https://developers.google.com/earth-engine/datasets/catalog/LANDSAT_LC08_C01_T1_TOA#bands.
[16] A. Sekertekin and S. Bonafoni, "Land surface temperature retrieval from Landsat 5, 7, and 8 over rural areas: Assessment of different retrieval algorithms and emissivity models and toolbox implementation," *Remote Sens.*, vol. **12**, no. 2, 2020, doi: 10.3390/rs12020294.
[17] Q. Vanhellemont, "Automated water surface temperature retrieval from Landsat 8/TIRS," *Remote Sens. Environ.*, vol. **237**, no. August 2019, p. 111518, 2020, doi: 10.1016/j.rse.2019.111518.

[18] NASA, "Landsat 7 (L7) Data Users Handbook," vol. **7**, no. November, p. 106, 2019, [Online]. Available: https://prd-wret.s3.us-west-2.amazonaws.com/assets/palladium/production/atoms/files/LSDS-1927_L7_Data_Users_Handbook-v2.pdf.
[19] U.S. Geological Survey, "Landsat 8 Data Users Handbook," *Nasa*, vol. **8**, no. June, p. 97, 2016, [Online]. Available: https://landsat.usgs.gov/documents/Landsat8DataUsersHandbook.pdf.
[20] G. Developer, "Sentinel-3 OLCI EFR: Ocean and Land Color Instrument Earth Observation Full Resolution," *Earth Engine Data Cat.*, 2020, [Online]. Available: https://developers.google.com/earth-engine/datasets/catalog/COPERNICUS_S3_OLCI#description.
[21] ESA, "OLCI Instrument Payload," *ESA Sentin. Online*, 2020, [Online]. Available: https://sentinels.copernicus.eu/web/sentinel/missions/sentinel-3/instrument-payload/olci.